



# CHORUS

This is the accepted manuscript made available via CHORUS. The article has been published as:

## Efficient charge generation from triplet excitons in metal-organic heterojunctions

Friedrich Roth, Stefan Neppl, Andrey Shavorskiy, Tiberiu Arion, Johannes Mahl, Hyun Ook Seo, Hendrik Bluhm, Zahid Hussain, Oliver Gessner, and Wolfgang Eberhardt

Phys. Rev. B **99**, 020303 — Published 7 January 2019

DOI: [10.1103/PhysRevB.99.020303](https://doi.org/10.1103/PhysRevB.99.020303)

# Efficient Charge Generation from Triplet Excitons in Metal-Organic Heterojunctions

Friedrich Roth,<sup>1,2</sup> Stefan Neppel,<sup>3†</sup> Andrey Shavorskiy,<sup>3§</sup> Tiberiu Arion,<sup>2¶</sup>  
Johannes Mahl,<sup>3</sup> Hyun Ook Seo,<sup>2‡</sup> Hendrik Bluhm,<sup>3</sup> Zahid Hussain,<sup>4</sup>  
Oliver Gessner,<sup>3\*</sup> and Wolfgang Eberhardt<sup>2,4,5\*</sup>

<sup>1</sup>Institute for Experimental Physics, TU Bergakademie Freiberg, D-09599 Freiberg, Germany

<sup>2</sup>Center for Free-Electron Laser Science / DESY, D-22607 Hamburg, Germany

<sup>3</sup>Chemical Sciences Division, Lawrence Berkeley National Laboratory, Berkeley, California 94720, USA

<sup>4</sup>Advanced Light Source, Lawrence Berkeley National Laboratory, Berkeley, California 94720, USA

<sup>5</sup>Institute of Optics and Atomic Physics, TU Berlin, D-10623 Berlin, Germany

Present addresses:

† Institute for Methods and Instrumentation for Synchrotron Radiation Research, Helmholtz-Zentrum Berlin für Materialien und Energie GmbH, 12489 Berlin, Germany

§ MAX IV Laboratory, Lund University, Lund, 221-00, Sweden

¶ P3 Systems GmbH, D-85055 Ingolstadt, Germany

‡ Department of Chemistry and Energy Engineering, Sangmyung University, Seoul 03016, Republic of Korea

---

\* corresponding authors, email: [ogessner@lbl.gov](mailto:ogessner@lbl.gov), [wolfgang.eberhardt@physik.tu-berlin.de](mailto:wolfgang.eberhardt@physik.tu-berlin.de)

## Abstract

The success of many emerging molecular electronics concepts hinges on an atomistic understanding of the underlying electronic dynamics. We employ picosecond time-resolved X-ray Photoemission Spectroscopy (tr-XPS) to elucidate the roles of singlet and triplet excitons for photoinduced charge generation at a copper-phthalocyanine – C<sub>60</sub> heterojunction. Contrary to common belief, fast intersystem crossing to triplet excitons after photoexcitation is not a loss channel but contributes to a significantly larger extent to the time-integrated interfacial charge generation than the initially excited singlet excitons. The tr-XPS data provide direct access to the diffusivity of the triplet excitons  $D_{CuPc} = (1.8 \pm 1.2) \times 10^{-5} \text{ cm}^2/\text{s}$  and their diffusion length  $L_{diff} = (8 \pm 3) \text{ nm}$ .

## Main Text

Metal-organic heterojunctions, such as metal-phthalocyanine (MePc) donor – C<sub>60</sub> acceptor systems [1-5], provide an important platform to advance understanding the electronic dynamics underlying many emerging molecular electronics concepts for photochemical and photovoltaic applications [6-16]. The prevailing picture for efficient charge generation is through singlet exciton dissociation at the donor-acceptor interface within less than 1 ps after photoexcitation in order to avoid photon energy loss to non-dissociating triplet excitons by fast intersystem crossing [17,18]. We employ picosecond time-resolved X-ray Photoemission Spectroscopy (tr-XPS), a technique of choice for measuring electronic structure with elemental and chemical site-specificity [19,20], to directly determine the triplet exciton diffusivity and the ratio of singlet and triplet exciton dissociation efficiencies in a copper-phthalocyanine (CuPc) – C<sub>60</sub> planar heterojunction (PHJ). Contrary to common belief, ultrafast intersystem crossing from

the initially excited singlet excitons to triplet excitons is not a loss channel but the long-lived triplet excitons contribute to a significantly larger extent to the time-integrated interfacial charge than the short-lived singlet excitons. The findings are important for tailoring organic heterojunction devices and provide a link between femtosecond-range interfacial and picosecond-to-nanosecond range bulk dynamics in organic semiconductors.

Optically induced charge transfer dynamics in MePc–C<sub>60</sub> heterojunctions are commonly initiated by HOMO-LUMO excitations of the MePc chromophore, followed by exciton delocalization and/or diffusion throughout the donor domain, charge separation at the MePc–C<sub>60</sub> interface and electron injection into C<sub>60</sub> LUMO polaron levels [1,3,4,8,10,15,16,18]. Based on extensive ultrafast optical transient absorption and 2-photon photoemission studies, a picture has emerged that charge generation in these systems occurs only within the first ~1 ps after photoexcitation and is to a large extent limited by efficient intersystem crossing from the initially excited singlet states to the lower-lying triplet state manifold followed by intramolecular recombination [2,17,18]. The short singlet state lifetimes in combination with an apparently strongly disfavored injection from triplet states and limited electronic coupling between bulk and interfacial donor molecules, has led to the suggestion that significant contributions to charge generation may be limited to only ~1-2 monolayers (MLs) of chromophores in immediate vicinity of the interface [17,18]. Since typical bulk heterojunction domain sizes are on the order of 10s of nm (i.e., 10s to ~100 MLs), this restriction seems to indicate a major, fundamental limitation to the amount of charge that may be generated from MePc–C<sub>60</sub> based heterojunction designs.

Here, we elucidate the roles of bulk and interfacial excitons for charge generation in MePc–C<sub>60</sub> heterojunctions by probing photoinduced electronic dynamics in planar bilayer

systems of CuPc and C<sub>60</sub> molecules using picosecond tr-XPS [19-21] (Fig. 1). Two types of CuPc–C<sub>60</sub> heterojunctions are studied under virtually identical experimental conditions. The first sample consists of ~2 MLs of C<sub>60</sub> deposited on top of ~5-20 MLs of CuPc (“C<sub>60</sub>/CuPc”), the

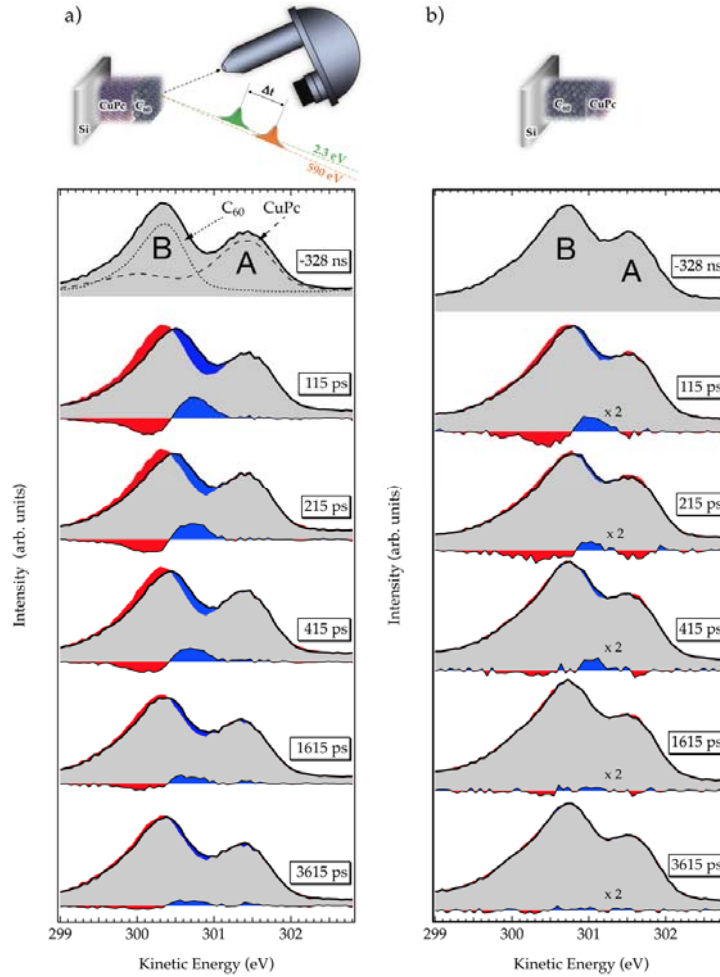


**Figure 1.** Time-resolved XPS spectra for planar heterojunction configurations of a) ~2 monolayers of C<sub>60</sub> deposited on top of a thin film of CuPc and b) ~2 monolayers of CuPc atop ~8 monolayers of C<sub>60</sub>. Pump-probe time delays are indicated in each panel. To highlight the photoinduced spectral changes, red and blue areas indicate missing and additional intensities, respectively, relative to the spectra recorded at a delay of -328 ns. Additionally, the difference spectra are shown and they are magnified by a factor of 2 in b). The dotted and dashed spectra in the -328 ns panel of a) are from pristine films of C<sub>60</sub> and CuPc, respectively. All films were supported by n-doped Si(100) substrates.

second sample of  $\sim 2$  MLs of CuPc atop  $\sim 8$  MLs of  $C_{60}$  (“CuPc/ $C_{60}$ ”). In both cases, n-doped Si(100) substrates are used to support the films and the bottom layer is prepared with sufficient thickness to eliminate XPS signal contributions from the interface with the Si substrate. The CuPc chromophores are excited using 10 ps long pump laser pulses with a center wavelength of 532 nm (2.3 eV photon energy). Electronic dynamics are probed by monitoring the time-dependent carbon K-shell photoemission from the samples, using  $\sim 70$  ps long X-ray pulses from the Advanced Light Source at a photon energy of 590 eV. See Sec. I and II of the Supplemental Material [22] for details of the sample preparation and the pump-probe experiment. Figures 1a and 1b show tr-XPS spectra of the  $C_{60}$ /CuPc and CuPc/ $C_{60}$  samples, respectively, at a variety of time delays as indicated. The spectra shown in the uppermost two panels of Fig. 1a are based on data previously presented in [19].

The ground state C 1s core level spectra recorded 328 ns before laser excitation agree qualitatively with previously recorded static C 1s spectra of the same system [38]. Two peaks with well-separated maxima at 301.4 eV (A) and 300.3 eV (B) kinetic energy are readily distinguished for the  $C_{60}$ /CuPc sample. Importantly, peak A is almost entirely associated with CuPc, while peak B is predominantly related to photoemission from  $C_{60}$  as indicated by the dashed and dotted spectra of the separate components in Fig. 1a, which were recorded using pristine films of CuPc and  $C_{60}$ , respectively [19]. The ground state C 1s binding energies associated with  $C_{60}$  and CuPc in the CuPc/ $C_{60}$  system are reduced by  $\approx 0.4$  eV and  $\approx 0.1$  eV, respectively, compared to the corresponding binding energies in the  $C_{60}$ /CuPc system. This is largely attributed to a static dipole shift between the two layers as previously reported for heterostructures [39] and ordered films [40]. In addition, there could also be a screening contribution from the Si substrate when it is in contact with the  $C_{60}$  film.

For both heterojunction configurations, the laser-induced dynamics only affect peak B, which exhibits a significant shift to higher kinetic energies upon excitation, while the binding energy of peak A remains constant. The shift of peak B is a signature of electron transfer from the chromophore CuPc to the electron acceptor C<sub>60</sub> and a reflection of the average concentration of charges within the C<sub>60</sub> domain, as described in our previous work [19]. A crucial observation is that the amplitude and temporal evolution of the C<sub>60</sub>-C1s photoline shift differ significantly for the two heterojunction configurations as illustrated in Fig. 2.

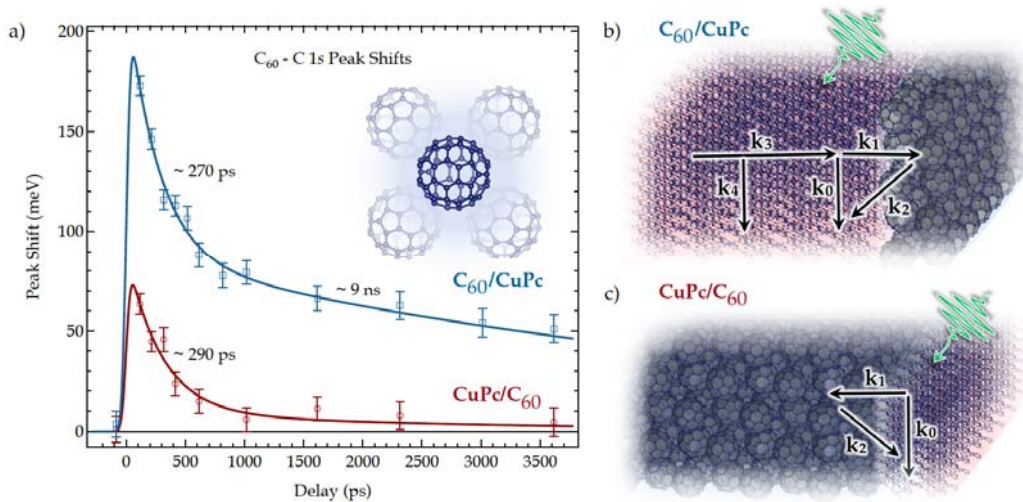


**Figure 2.** a) Temporal evolution of C<sub>60</sub> - C 1s peak shift for C<sub>60</sub>/CuPc (blue squares) and CuPc/C<sub>60</sub> (red circles) heterojunctions. Symbols and error bars indicate measurements with  $\pm 1\sigma$  uncertainties. Solid lines are the result of a fit to a coupled rate equation model taking into account the energy- and charge-transfer processes indicated in b) and c). Note that only  $\tau_2 = 1/k_2 = (280 \pm 40)$  ps and  $\tau_3 = 1/k_3 = (9 \pm 4)$  ns are derived from the fit while all other rates are known from literature. See text for details.

Blue squares and red circles in Fig. 2a correspond to the time-dependent shifts of the C<sub>60</sub>-C1s photoline for C<sub>60</sub>/CuPc and CuPc/C<sub>60</sub> samples, respectively. For both PHJ arrangements, the C<sub>60</sub> peak in the excited systems is shifted to higher kinetic energies, i.e., lower binding

energies. The extent, however, of the transient peak shifts and, in particular, their dynamic evolution differ significantly. For the  $C_{60}/CuPc$  system, peak B shifts towards higher kinetic energies by  $\approx 170$  meV immediately after optical excitation while the  $CuPc/C_{60}$  system exhibits a much smaller maximum peak shift of only  $\sim 65$  meV. In both cases, the shift decreases rapidly within a few hundred picoseconds after excitation. On longer timescales, a long-lived dynamic component is very prominent in the  $C_{60}/CuPc$  system but virtually absent in the  $CuPc/C_{60}$  system.

We note that both  $CuPc$  and  $C_{60}$  absorb at 2.3 eV photon energy and, thus, the pump pulse induces electronic excitations in both domains. However, as discussed in more detail in Sec. IV of the Supplemental Material [22], the site-specific photoline shift is predominantly associated with core-hole screening effects by delocalized charges in the  $C_{60}$  acceptor domain after electron injection from the  $CuPc$  donor [19]. The peak shift is, therefore, a site-specific probe of the average amount of injected charge per  $C_{60}$  molecule. Neither a pristine  $CuPc$  nor a pristine  $C_{60}$  film deposited on the Si(100) substrate exhibits any photo-induced peak shifts beyond the independently quantified photovoltage response of the n-doped substrate [19]. This strongly suggests that CT dynamics at both the  $CuPc/Si$  and the  $C_{60}/Si$  interface are of minor importance for the processes discussed herein. Instead, electronic dynamics within the organic donor/acceptor system must be responsible for the observed trends. In order to interpret the evolution of the average charge within the  $C_{60}$  acceptor phase for both heterojunction configurations within a consistent physical picture, we employ a set of 1<sup>st</sup> order coupled rate equations based on the model illustrated in Fig. 2b.

Within this model, the rates  $k_i$  are associated with the following processes: intramolecular relaxation back to the ground state within interfacial donors ( $k_0$ ), charge injection from excited

interfacial donors ( $k_1$ ), interfacial acceptor-donor electron-hole recombination ( $k_2$ ), exciton migration from the donor bulk to interfacial layers ( $k_3$ ), and relaxation to the ground state within the donor bulk ( $k_4$ ). The comprehensive literature on relaxation dynamics in CuPc and CuPc–C<sub>60</sub> systems together with self-consistency arguments provides all but two of the five rate constants in Fig. 2b (see Sec. III of the Supplemental Material [22] for details). The remaining two rates,  $k_2$  and  $k_3$  are derived from a well-defined fit of both, the C<sub>60</sub>/CuPc and CuPc/C<sub>60</sub> data sets as represented by the blue and red solid lines, respectively, in Fig. 2a.

The procedure reveals the timescales for exciton bulk-to-interface migration  $\tau_3 = 1/k_3 = (9 \pm 4)$  ns and for interfacial electron-hole recombination  $\tau_2 = 1/k_2 = (280 \pm 40)$  ps. The differences between the dynamic trends observed in the two bi-layer systems follow naturally from the described model. With only  $\sim 2$  MLs of CuPc in the CuPc/C<sub>60</sub> system, contributions of the slow bulk component to the transients are strongly suppressed while the interfacial electron-hole recombination rate is similar for both systems (Fig. 2c). Note that no bias voltage has been applied in this study. Thus, injected charges are not expected to migrate far away from the interface due to their Coulomb interaction with holes in the donor. Nevertheless, the average amount of injected charge per C<sub>60</sub> molecule is expected to be higher for the C<sub>60</sub>/CuPc system as compared to the CuPc/C<sub>60</sub> system at any given time due to the different ratios of donor and acceptor molecules within the photo-active regions of the samples. This may explain the different amplitudes of the C<sub>60</sub>-C1s peak shifts for the two different sample configurations.

Comparison of the intersystem crossing time of  $\approx 500$  fs in CuPc [5,17,18] with the 9 ns average excitation transfer time within the CuPc domain strongly suggests that the vast majority of donor states contributing to the long-term charge component must have relaxed to the triplet manifold. Based on ultrafast measurements on few-monolayer systems and energy

considerations, injection from these states is generally considered extremely disfavored [17,18]. However, using a combination of several complementary spectroscopic techniques, Piersimoni *et al.* found that interfacial triplet excitons in a CuPc–C<sub>60</sub> PHJ may dissociate into separate charges with an efficiency comparable to that of singlet exciton dissociation in a metal-free H<sub>2</sub>Pc–C<sub>60</sub> PHJ [41]. The results presented here are consistent with these findings and suggest that for extended CuPc donor structures, injection from triplet excitons is actually the dominant charge generation pathway while for few-monolayer structures it is much less prominent since it cannot compete with the significantly faster interfacial dynamics. Note that the exact mechanism for charge injection from triplet excitons is unknown and the rate may have any value  $\gg(100 \text{ ps})^{-1}$  [17,41]. However, as discussed in Sec. III of the Supplemental Material [22], this does not affect the conclusions presented above and, for simplicity, the same injection rate is applied for singlet and triplet excitons.

Due to the sensitivity of the tr-XPS experiment to both singlet and triplet exciton dissociation at the interface, the ratio of charge generation from both types of excitation can be directly determined. A component analysis of the fit in Fig. 2a suggests that bulk triplet states generate approximately ten times more charges in the acceptor than interfacial singlet states for the C<sub>60</sub>/CuPc sample. In other words, on ultrafast timescales, injection from interfacial singlet states is the dominating charge generation mechanism. On longer timescales, however, and in application-like, extended donor-acceptor systems, the integrated charge generated from bulk triplet states is significantly larger. These findings are illustrated in Fig. 3. It shows the calculated time-dependent contributions of singlet and triplet exciton dissociation to interfacial charge generation as blue- and red-shaded curves, respectively. Note that interfacial charge-transfer (ICT) states may be transiently populated as well, but cannot be detected in the experiment due

to their short ( $\approx 1$  ps) lifetimes [17,18].

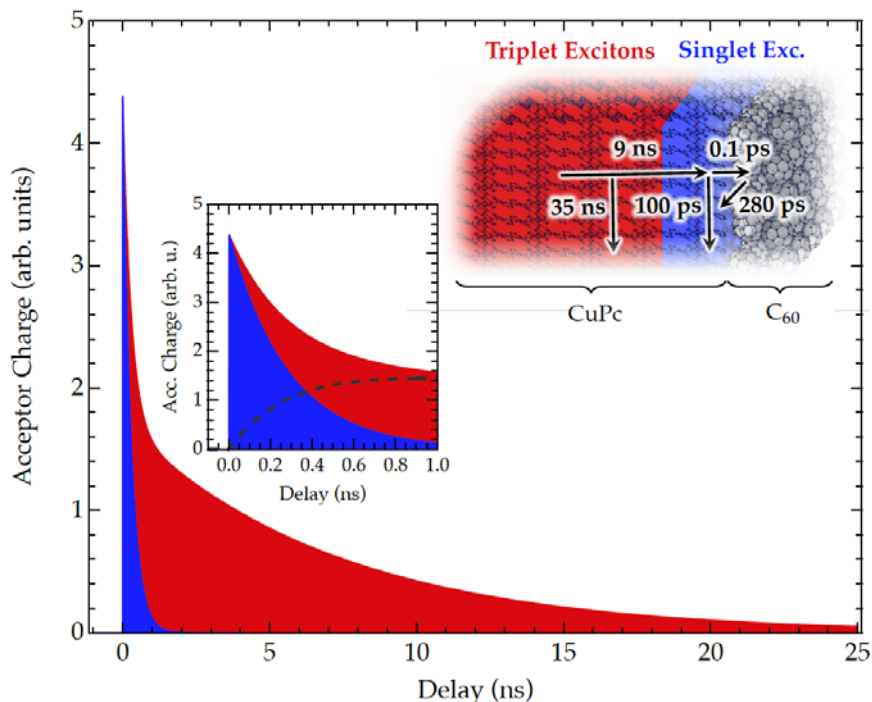


**Figure 3.** Photoinduced charge generation in a planar CuPc–C<sub>60</sub> heterojunction. Blue and red shaded areas correspond to the time-dependent contributions to the acceptor charges from singlet and triplet exciton splitting, respectively. The triplet exciton contribution is also plotted separately as a dashed line in the inset.

The maximum amount of charges that may be created via the triplet channel is given by the ratio of the bulk triplet exciton transport rate and the bulk triplet relaxation rate. This is the well-known “rule of thumb” for the design of bulk heterojunctions that requires the typical dimension of the donor phase to be on the order of the exciton diffusion length  $L_{diff}$ , i.e., the distance an exciton may migrate during its lifetime. Any larger donor domains lead to a lower light-to-charge conversion efficiency as absorbed photon energy is increasingly lost to exciton recombination.

In order to gain deeper physical insight into the charge carrier dynamics, we analyze the

tr-XPS results based on established models for energy transfer in organic semiconductors as well as previously determined exciton diffusion lengths. The timescale  $\tau$  for exciton diffusion across a distance  $L$  is given by

$$\tau = \frac{L^2}{D} \quad (1)$$

where  $D$  is the diffusion coefficient (diffusivity) that describes the mobility of excitons inside a material [8,17]. Exciton diffusion in organic semiconductor films proceeds via different mechanisms for singlet and triplet excitons. Singlet excitons migrate via Förster resonant energy transfer, triplet excitons via Dexter energy transfer [42-44]. The diffusion coefficients  $D_D$  and  $D_F$  associated with Dexter and Förster type energy transport, respectively, usually differ significantly with  $D_D \ll D_F$ . Nevertheless, typical diffusion lengths of triplet excitons are often comparable to those of singlet excitons due to orders of magnitude longer triplet lifetimes [42,43,45]. With an average diffusion distance  $L = (4 \pm 1)$  nm from the CuPc bulk to the C<sub>60</sub>/CuPc interface and an average diffusion timescale of  $\tau_3 = k_3^{-1} = (9 \pm 4)$  ns, Eq. (1) yields a diffusion coefficient for exciton migration in the CuPc domain of  $D_{CuPc} = (1.8 \pm 1.2) \times 10^{-5}$  cm<sup>2</sup>/s. To the best of our knowledge, this is the first direct experimental determination of the exciton diffusivity within a CuPc donor domain.

The magnitude of  $D_{CuPc}$  is quite small for organic semiconductors, as expected for triplet exciton diffusion [42]. While there are no CuPc diffusivity values available to directly compare the tr-XPS result with, several studies measured the exciton diffusion length of CuPc, yielding typical values for  $L_{diff}$  between 5 nm and 10 nm [41,46-49]. Combined with measured triplet exciton lifetimes between ~9 ns and 35 ns [5,50], the range of possible CuPc diffusivities may be estimated by Eq. (1) to  $D_{CuPc} \sim (0.7-11) \times 10^{-5}$  cm<sup>2</sup>/s. The diffusivity determined here is clearly within these boundaries but the direct access to the quantity in the tr-XPS experiment improves

its accuracy significantly. Vice versa, the diffusion coefficient  $D_{CuPc}$  determined here and an exciton lifetime of 35 ns, as employed in the rate equation analysis, correspond to a diffusion length of  $L_{diff} = (8 \pm 3)$  nm, in good agreement with most other measurements [41,46-48].

We note that alternative relaxation mechanisms have been examined but were found to be incompatible with the observed tr-XPS trends. Bartelt *et al.* observed nanosecond-range decay timescales in optically excited ZnPc/C<sub>60</sub> blends using transient THz spectroscopy [4]. The slowly decaying photoconductivity of the samples was interpreted as the signature of a diminishing electron concentration in the C<sub>60</sub> phase due to nanosecond-scale recombination dynamics. In the case of the two heterojunction systems studied here, this interpretation is not applicable since it does not explain the vanishing long-term component in the CuPc/C<sub>60</sub> system. In fact, if the long-term component were associated with recombination dynamics, it would be expected to be more pronounced for the CuPc/C<sub>60</sub> system since the electrons would probably spend more time in the more extended C<sub>60</sub> acceptor phase compared to the C<sub>60</sub> double-layer of the C<sub>60</sub>/CuPc system.

We have also considered the possibility that charge-transfer dynamics at the interface between the molecular films and the Si substrate may have an impact on the measurements. However, as noted above, neither a pristine film of CuPc nor a pristine film of C<sub>60</sub> deposited on the substrate exhibits any peak shifts beyond the independently measured photovoltage response of the n-doped Si wafer [19]. This observation strongly suggests a minor role of CT between the Si substrate and the molecular adsorbates. We, nevertheless, evaluated the concept that the slow component in the C<sub>60</sub>-C1s peak shifts may be associated with discharging of the C<sub>60</sub> electron acceptor instead of exciton transport in the CuPc electron donor. In this case, the key idea to explain the lack of the long-term component in the CuPc/C<sub>60</sub> sample would be a more efficient charge extraction from the C<sub>60</sub> domain across two interfaces (C<sub>60</sub>-Si and C<sub>60</sub>-CuPc) for the

CuPc/C<sub>60</sub> sample compared to just one C<sub>60</sub>-CuPc interface for the C<sub>60</sub>/CuPc sample. However, this scenario would lead to two different mono-exponential decay trends for the two sample configurations instead of the observed bi-exponential decays with varying relative contributions of slow and fast dynamics.

Note that the new insight into the charge carrier generation dynamics in this heterojunction system has been enabled by the ability to simultaneously determine both the length- and timescales of triplet exciton migration. The length-scale is defined by the sample preparation and characterization technique and the timescale is accessible through the simultaneous temporal sensitivity and site-specificity of the X-ray probing technique. The experiment also gives direct access to the timescale for interfacial electron-hole recombination  $1/k_2 = (280 \pm 40)$  ps at the CuPc-C<sub>60</sub> interface, which is on the same order of magnitude as recombination timescales in other organic heterojunction systems employing fullerene-based acceptors [51,52]. The amount of information on interfacial energy- and charge-transfer dynamics gained in a single tr-XPS experiment is quite remarkable. Future studies will take advantage of this newly gained capability and translate it to even more extensive temporal and spatial scales. In particular, next generation high repetition rate X-ray free electron laser light sources such as the European XFEL and LCLS II will provide excellent conditions to expand the reach of the method into the femtosecond domain such that virtually all relevant rates across multiple scales can be determined by a series of experiments at a single light source.

### **Acknowledgments**

This work was supported within the program 'Structure of Matter' of the Helmholtz Association and by the Director, Office of Science, Office of Basic Energy Sciences, Division of

Chemical Sciences, Geosciences, and Biosciences of the US Department of Energy at the Lawrence Berkeley National Laboratory under Contract No. DE-AC02-05CH11231. OG was supported by the Department of Energy Office of Science Early Career Research Program. FR acknowledges financial support by the VI 419 of the Helmholtz Association. SN acknowledges support by the Alexander von Humboldt foundation. JM acknowledges support from the ALS Doctoral Fellowship in Residence Program. We would like to thank the staff at the Advanced Light Source (ALS) for their excellent support during the experiment. The ALS is supported by the Director, Office of Science, Office of Basic Energy Sciences, of the U.S. Department of Energy under Contract No. DE-AC02-05CH11231. The Molecular Environmental Sciences beamline 11.0.2 is supported by the Director, Office of Science, Office of Basic Energy Sciences, and the Division of Chemical Sciences, Geosciences, and Biosciences of the US Department of Energy at the Lawrence Berkeley National Laboratory under Contract No. DE-AC02-05CH11231. WE would like to thank the ALS for their support and hospitality.

## References

- [1] G. J. Dutton, W. Jin, J. E. Reutt-Robey, and S. W. Robey, *Phys. Rev. B* **82**, 073407 (2010).
- [2] G. J. Dutton and S. W. Robey, *J. Phys. Chem. C* **117**, 25414 (2013).
- [3] N. Sai, R. Gearba, A. Dolocan, J. R. Tritsch, W.-L. Chan, J. R. Chelikowsky, K. Leung, and X. Zhu, *J. Phys. Chem. Lett.* **3**, 2173 (2012).
- [4] A. F. Bartelt, C. Strothka, M. Pempfer, W. Schindler, K. Fostiropoulos, and R. Eichberger, *Appl. Phys. Lett.* **99**, 143304 (2011).
- [5] B. W. Caplins, T. K. Mullenbach, R. J. Holmes, and D. A. Blank, *Phys. Chem. Chem. Phys.* **18**, 11454 (2016).
- [6] N. S. Sariciftci, L. Smilowitz, A. J. Heeger, and F. Wudl, *Science* **258**, 1474 (1992).
- [7] S. Günes, H. Neugebauer, and N. S. Sariciftci, *Chem. Rev.* **107**, 1324 (2007).
- [8] J.-L. Brédas, J. E. Norton, J. Cornil, and V. Coropceanu, *Acc. Chem. Res.* **42**, 1691 (2009).
- [9] J. Piris, T. E. Dykstra, A. A. Bakulin, P. H. M. v. Loosdrecht, W. Knulst, M. T. Trinh, J. M. Schins, and L. D. A. Siebbeles, *J. Phys. Chem. C* **113**, 14500 (2009).
- [10] T. M. Clarck and J. R. Durrant, *Chem. Rev.* **110**, 6736 (2010).
- [11] Y. Sun, G. C. Welch, W. L. Leong, C. J. Takacs, G. C. Bazan, and A. J. Heeger, *Nat. Mater.* **11**, 44 (2012).
- [12] C. S. Ponseca, P. Chábera, J. Uhlig, P. Persson, and V. Sundström, *Chem. Rev.* **117**, 10940 (2017).
- [13] A. C. Jakowetz, M. L. Böhm, A. Sadhanala, S. Huettner, A. Rao, and R. H. Friend, *Nat. Mater.* **16**, 551 (2017).
- [14] K. Nakano and K. Tajima, *Adv. Mater.* **29**, 1603269 (2017).
- [15] X. Y. Zhu, Q. Yang, and M. Muntwiler, *Acc. Chem. Res.* **42**, 1779 (2009).

- [16] L. G. Kaake, J. J. Jasieniak, R. C. Bakus, G. C. Welch, D. Moses, G. C. Bazan, and A. J. Heeger, *J. Am. Chem. Soc.* **134**, 19828 (2012).
- [17] G. J. Dutton and S. W. Robey, *J. Phys. Chem. C* **116**, 19173 (2012).
- [18] A. E. Jailaubekov, A. P. Willard, J. R. Tritsch, W.-L. Chan, N. Sai, R. Gearba, L. G. Kaake, K. J. Williams, K. Leung, P. J. Rossky, and X. Y. Zhu, *Nat. Mater.* **12**, 66 (2013).
- [19] T. Arion, S. Neppl, F. Roth, A. Shavorskiy, H. Bluhm, Z. Hussain, O. Gessner, and W. Eberhardt, *Appl. Phys. Lett.* **106**, 121602 (2015), *Appl. Phys. Lett.* **107**, 019903 (2015).
- [20] S. Neppl and O. Gessner, *J. Electron. Spectrosc. Relat. Phenom.* **200**, 64 (2015).
- [21] S. Neppl, A. Shavorskiy, I. Zegkinoglou, M. W. Fraund, D. Slaughter, T. Troy, M. P. Ziemkiewicz, M. Ahmed, S. Gul, B. Rude, J. Z. Zhang, A. S. Tremsin, P.-A. Glans, Y.-S. Liu, C. H. Wu, J. Guo, M. Salmeron, H. Bluhm, and O. Gessner, *Faraday Discuss.* **171**, 219 (2014).
- [22] See Supplemental Material at [URL will be inserted by publisher] for details on (I) sample preparation, (II) pump-probe experiment, (III) data analysis, and (IV) excitations and line shifts, which includes Refs. [23-37].
- [23] H. Bluhm *et al.*, *J. Electron. Spectrosc. Relat. Phenom.* **150**, 86 (2006).
- [24] A. Shavorskiy *et al.*, *Rev. Sci. Instrum.* **85**, 093102 (2014).
- [25] T. E. Glover, G. D. Ackermann, A. Belkacem, B. Feinberg, P. A. Heimann, Z. Hussain, H. A. Padmore, C. Ray, R. W. Schoenlein, and W. F. Steele, *Nucl. Instrum. Meth. A* **467-468**, 1438 (2001).
- [26] I. G. Hill, A. Kahn, Z. G. Soos, and Pascal, Jr., *Chem. Phys. Lett.* **327**, 181 (2000).
- [27] O. Esenturk, J. S. Melinger, P. A. Lane, and E. J. Heilweil, *J. Phys. Chem. C* **113**, 18842 (2009).
- [28] A. L. Ayzner, D. Nordlund, D.-H. Kim, Z. Bao, and M. F. Toney, *J. Phys. Chem. Lett.* **6**, 6 (2015).
- [29] H. Dong, H. Zhu, Q. Meng, X. Gong, and W. Hu, *Chem. Soc. Rev.* **41**, 1754 (2012).
- [30] X. Li, Y. Chen, J. Sang, B.-X. Mi, D.-H. Mu, Z.-G. Li, H. Zhang, Z.-Q. Gao, and W. Huang, *Org. Electron.* **14**, 250 (2013).
- [31] W. Widdra, D. Bröcker, T. Gießel, I. V. Hertel, W. Krüger, A. Liero, F. Noack, V. Petrov, D. Pop, P. M. Schmidt, R. Weber, I. Will, and B. Winter, *Surf. Sci.* **543**, 87 (2003).
- [32] A. Pietzsch, A. Föhlisch, F. Hennies, S. Vijayalakshmi, and W. Wurth, *Appl. Phys. A* **88**, 587 (2007).
- [33] K. R. Siefertmann *et al.*, *J. Phys. Chem. Lett.* **5**, 2753 (2014).
- [34] H. Dachraoui, M. Michelswirth, P. Siffalovic, P. Bartz, C. Schäfer, B. Schnatwinkel, J. Mattay, W. Pfeiffer, M. Drescher, and U. Heinzmann, *Phys. Rev. Lett.* **106**, 107401 (2011).
- [35] R. Jacquemin, S. Kraus, and W. Eberhardt, *Solid State Commun.* **105**, 449 (1998).
- [36] S. Link, A. Scholl, R. Jacquemin, and W. Eberhardt, *Solid State Commun.* **113**, 689 (2000).
- [37] H. Yagi, K. Nakajima, K. R. Koswattage, K. Nakagawa, C. Huang, M. S. I. Proshan, B. P. Kafle, H. Katayanagi, and K. Mitsuke, *Carbon* **47**, 1152 (2009).
- [38] B. Kessler, *Appl. Phys. A* **67**, 125 (1998).
- [39] F. Roth, C. Lupulescu, T. Arion, E. Darlatt, A. Gottwald, and W. Eberhardt, *J. Appl. Phys.* **115**, 033705 (2014).
- [40] O. V. Molodtsova and M. Knupfer, *J. Appl. Phys.* **99**, 053704 (2006).
- [41] F. Piersimoni, D. Cheyns, K. Vandewal, J. V. Manca, and B. P. Rand, *J. Phys. Chem. Lett.* **3**, 2064 (2012).
- [42] R. R. Lunt, N. C. Giebink, A. A. Belak, J. B. Benziger, and S. R. Forrest, *J. Appl. Phys.* **105**, 053711 (2009).
- [43] P. Heremans, D. Cheyns, and B. P. Rand, *Acc. Chem. Res.* **42**, 1740 (2009).
- [44] O. V. Mikhnenko, P. W. M. Blom, and T.-Q. Nguyen, *Energy Environ. Sci.* **8**, 1867 (2015).
- [45] Y. Shao and Y. Yang, *Adv. Mater.* **17**, 2841 (2005).
- [46] T. K. Mullenbach, I. J. Curtin, T. Zhang, and R. J. Holmes, *Nat. Commun.* **8**, ncomms14215 (2017).
- [47] M. Ichikawa, *Thin Solid Films* **527**, 239 (2013).
- [48] P. Peumans, A. Yakimov, and S. R. Forrest, *J. Appl. Phys.* **93**, 3693 (2003).
- [49] T. Stübinger and W. Brütting, *J. Appl. Phys.* **90**, 3632 (2001).
- [50] J. McVie, R. S. Sinclair, and T. G. Truscott, *J. Chem. Soc., Faraday Trans. 2* **74**, 1870 (1978).
- [51] I.-W. Hwang, D. Moses, and A. J. Heeger, *J. Phys. Chem. C* **112**, 4350 (2008).
- [52] J. Guo, H. Ohkita, H. Benten, and S. Ito, *J. Am. Chem. Soc.* **132**, 6154 (2010).